

Supplemental figures

Figure S1. Impact of pMHCII stability on the accumulation of CD44^{hi}CD62L^{hi} antigen-specific CD4 T cells

(A) As displayed in Figure 2, antigen-specific CD4 T cells ($V\alpha 11^+V\beta 3^+CD44^{hi}CD62L^{hi}$) at day 7 in LN from B10.BR mice immunized with the indicated peptide. Profiles are pre-gated on DAPI negative cells that are $B220^-CD8^-CD11b^-$ and $V\alpha 11^+V\beta 3^+$. Numbers above boxed areas indicate percent cells in profile. (B) Total number of CD44^{hi}CD62L^{hi} antigen-specific CD4 T cells 7 days after immunization with the indicated peptide. Data shown are derived from three independent experiments (mean \pm SEM; $n \geq 3$ mice per group).

Figure S2. Impact of pMHCII stability on TCR α chain selection

Antigen-driven selection for preferred CDR3 features in α -chain of the TCR. Single antigen-specific CD4 T cells ($V\alpha 11^+V\beta 3^+CD44^{hi}CD62L^{lo}$) were sorted from draining lymph nodes of B10.BR mice immunized with the indicated peptide. Single-cell repertoire analysis was done as described in Materials and Methods. Each dot represents the sequence information from a single-cell. The y-axis represents (A) J α usage (B) CDR3 α length in number of amino acids (aa) (C) aa present at position $\alpha 93$, and (D) $\alpha 95$. The numbers of sequences used in the analysis are displayed (across three separate mice for each condition). Data shown are derived from three independent experiments (3 mice per group).

Figure S3. Impact of pMHCII stability on TCR β chain selection

Antigen-driven selection for preferred CDR3 features in β -chain of the TCR. Single antigen-specific CD4 T cells ($V\alpha 11^+V\beta 3^+CD44^{hi}CD62L^{lo}$) were sorted from draining LN of B10.BR mice immunized with the indicated peptide. Single-cell repertoire analysis was done as described in Materials and Methods. Each dot represents the sequence information from a single-cell. The y-axis represents (A) J β usage, (B) aa present at position $\beta 102$, (C) the CDR3 β length in number of aa, and (D) aa present at position $\beta 100$. The numbers of sequences used in the analysis are displayed (across three separate mice for each condition). Data shown are derived from three independent experiments ($n \geq 3$ mice per group).

Figure S4. Impact of pMHCII stability on TCR β chain selection

All TCR β amino acid sequences of antigen-specific CD4 T cells ($V\alpha 11^+V\beta 3^+CD44^{hi}CD62L^{lo}$) analyzed in this study. Frequency of TCR β public, recurrent and private amino acid sequences in antigen-specific CD4 T cells sorted from draining LN of B10.BR mice immunized with the indicated peptide are depicted. Data shown are derived from three independent experiments (means \pm SEM; $n \geq 3$ mice per group).

Figure S5. TCR binding properties of PCC-specific TCR $\alpha\beta$ transgenic cells

Peptide-MHCII tetramer staining and TCR $V\alpha 11$ expression levels of CD4 T cells isolated from LN of naïve AND $\alpha\beta$ (CDR3 β : SLNNANSDY, J $\beta 1.2$) and low affinity

2B4 $\alpha\beta$ (CDR3 β : SLNWSQDTQ, J β 2.5) (14) PCC-specific TCR transgenic mice. Mean fluorescence intensity of **(A)** pMHCII tetramer staining and **(B)** V α 11 expression of indicated TCR $\alpha\beta$ cells. Representative histograms of two independent experiments are shown.

Figure S6. Antigen dose impacts clonotypic diversity

Single-cell repertoire analysis of individual antigen-specific CD4 T cells (V α 11⁺V β 3⁺CD44^{hi}CD62L^{lo}) sorted from mice immunized with the indicated dose of PCC_{103K}. **(A-C)** Average number \pm SEM of preferred CDR3 features per cell for the **(A)** whole TCR, **(B)** TCR α chain only or **(C)** TCR β chain only. *, $P \leq 0.05$, between indicated peptides (unpaired Student's t-test). Data shown are derived from three independent experiments ($n \geq 3$ mice per group).

Figure S1

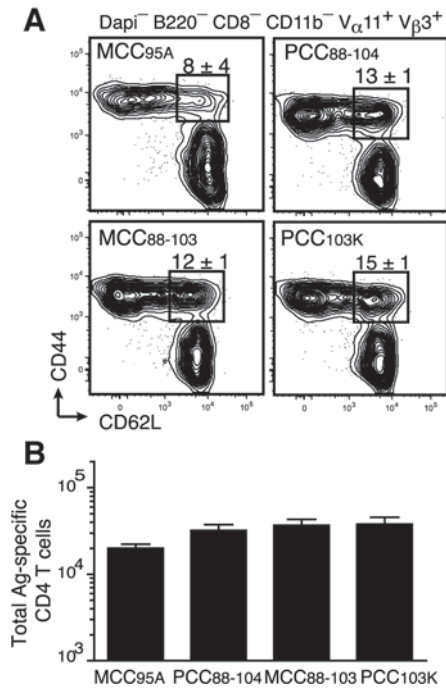
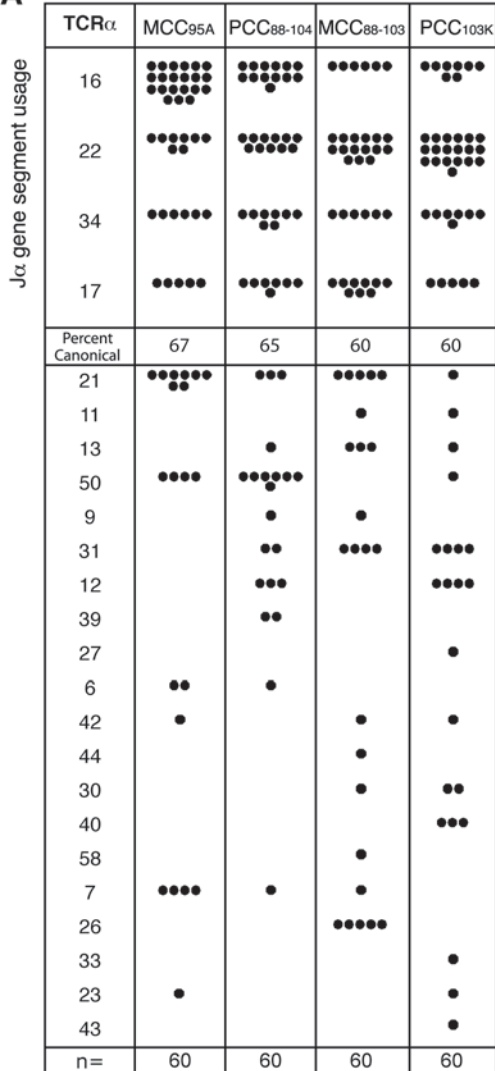
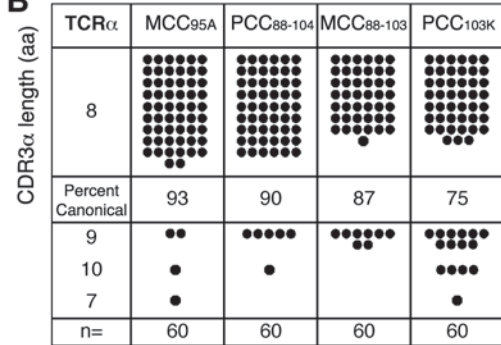


Figure S2

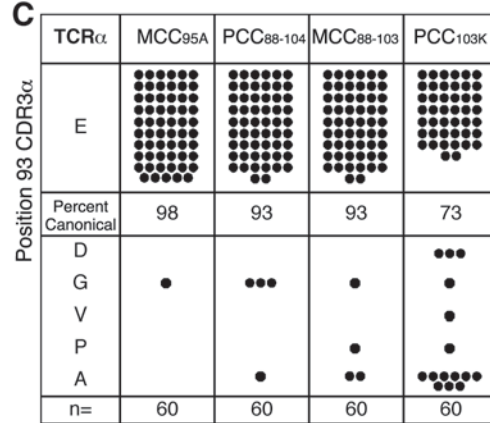
A



B



C



D

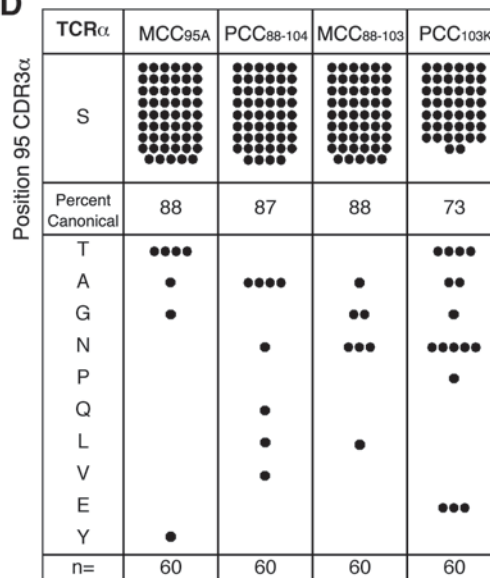
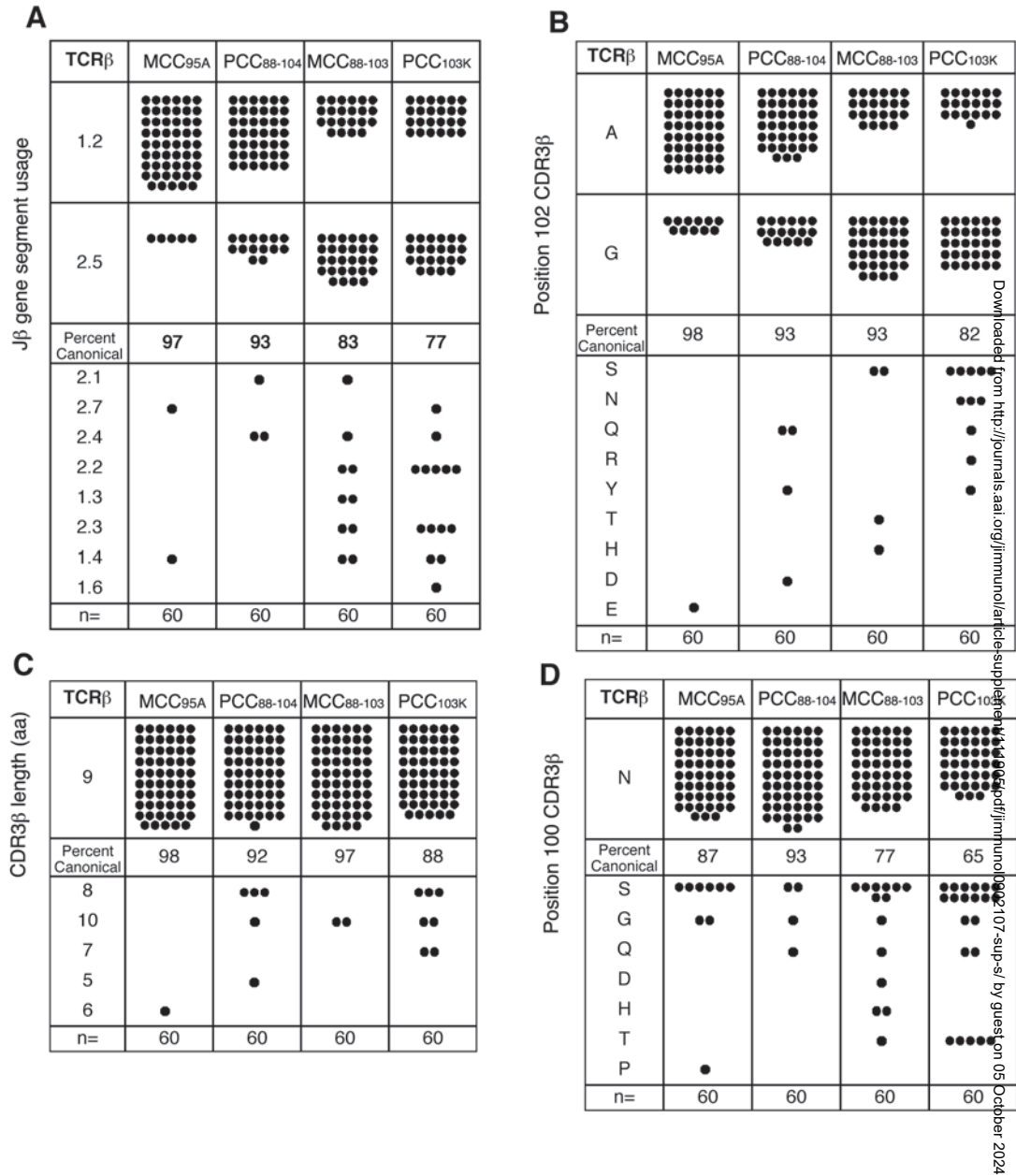


Figure S3



Downloaded from http://journals.aai.org/immunology/advance-article/doi/10.1093/immunology/ckad007/6545494 by guest on 05 October 2024

Figure S4

CDR3 β Loop	J β	MCC95A	PCC88-104	MCC88-103	PCC103K
SLNNA NSDY	1.2				
SLNSA NSDY	1.2				
SLNRGQDTQ	2.5				
Public		75 \pm 8	73 \pm 8	52 \pm 4	22 \pm 7
SLSAGRS DY	1.2				
SLSSGRS DY	1.2				
SLNRANS DY	1.2				
SLNWGEDTQ	2.5				
SLNWGQDTQ	2.5				
SLSTGTGQL	2.2				
SPNRGQDTQ	2.5				
SPNNA NSDY	1.2				
Recurrent		12 \pm 2	8 \pm 4	22 \pm 3	15 \pm 5
SLNRGS DTQ	2.5				
SLNWGDDTQ	2.5				
IRGREG	2.7				
SSGGANS DY	1.2				
SLNAGDSDY	1.2				
SLPGANERL	1.4				
SLNGGGS DY	1.2				
SLNSDY	1.2				
SLSAGI SDY	1.2				
SLNRGVDTQ	2.5				
SLNWGGGDTQ	2.5				
SLNWGVDTQ	2.5				
SPNWGKDTQ	2.5				
SLSQQDTQ	2.5				
RGQGYAEQ	2.1				
SPGRQNTL	2.4				
SQNWGENEQ	2.4				
SPHRGRAETL	2.3				
SLNSGNSDY	1.2				
SLSHANS DY	1.2				
SLSTGVSDY	1.2				
SLNGGQDTQ	2.5				
SRNWGQDTQ	2.5				
SRNRGQDTQ	2.5				
SRQGAGDTQ	2.5				
SLSYGQDTQ	2.5				
SLSTGTGNTL	1.3				
SLSTSGNTL	1.3				
LSWANERL	1.4				
LSWGHHERL	1.4				
SPDSHYAEQ	2.1				
SLGHSQNTL	2.4				
SLNWGTETL	2.3				
SLNWGKDTQ	2.5				
GQTNSDY	1.2				
SPNWGQDTQ	2.5				
SLSSGVDTQ	2.5				
SLNFANS DY	1.2				
SLNYANS DY	1.2				
SLNRRDS DY	1.2				
SLSQGRSDY	1.2				
SLSSANS DY	1.2				
SLNMA NSDY	1.2				
SLSTGANS DY	1.2				
SPGQGGSDY	1.2				
SWTGNSDY	1.2				
SSTGNSDY	1.2				
SQNSANADY	1.2				
SLNLGQDTQ	2.5				
SLNTAQDTQ	2.5				
SLNRAQDTQ	2.5				
SLNTGQDTQ	2.5				
SPQGAQDTQ	2.5				
SPQGGQDTQ	2.5				
SLSTGVDTQ	2.5				
SLNFSNERL	1.4				
SLTFSNERL	1.4				
SLSGYNSPL	1.6				
SLSTGHTGQL	2.2				
SRDSNTQL	2.2				
SLSTGAETL	2.3				
SPGSQNTL	2.4				
SLNWGGGEQ	2.7				
Private		13 \pm 7	18 \pm 4	27 \pm 6	63 \pm 12
n=		60	60	60	60

Downloaded from <http://journals.aai.org/jimmunol/article-supplement/11305.pdf/jimmunol090217> by guest on 05 October 2024

Figure S5

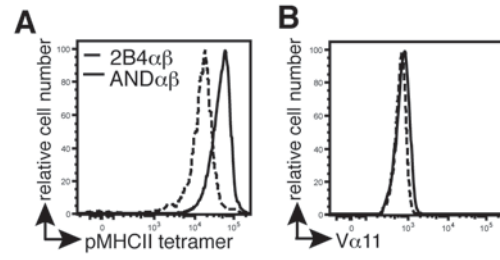


Figure S6

